Abnormal B cell memory subsets dominate HIV-specific responses in infected individuals

Lela Kardava,[1] Susan Moir,[1] Naisha Shah,[2] Wei Wang,[1] Richard Wilson,[3] Clarisa M. Buckner,[1] Brian H. Santich,[1] Leo J.Y. Kim,[1] Emily E. Spurlin,[1] Amy K. Nelson,[1] Adam K. Wheatley,[4] Christopher J. Harvey,[5] Adrian B. McDermott,[4] Kai W. Wucherpfennig,[5,6] Tae-Wook Chun,[1] John S. Tsang,[2,7] Yuxing Li,[3,4,8] and Anthony S. Fauci[1]

[1]Laboratory of Immunoregulation and [2]Systems Genomics and Bioinformatics Unit of Laboratory of Systems Biology, National Institute of Allergy and Infectious Diseases (NIAID), NIH, Bethesda, Maryland, USA. [3]International AIDS Vaccine Initiative Neutralizing Antibody Center at The Scripps Research Institute, La Jolla, California, USA. [4]Vaccine Research Center, NIAID, NIH, Bethesda, Maryland, USA. [5]Department of Cancer Immunology and AIDS, Dana-Farber Cancer Institute, and [6]Program in Immunology, Harvard Medical School, Boston, Massachusetts, USA. [7]Trans-NIH Center for Human Immunology, NIH, Bethesda, Maryland, USA. [8]Department of Immunology and Microbial Science, The Scripps Research Institute, La Jolla, California, USA.

Recently, several neutralizing anti-HIV antibodies have been isolated from memory B cells of HIV-infected individuals. Despite extensive evidence of B cell dysfunction in HIV disease, little is known about the cells from which these rare HIV-specific antibodies originate. Accordingly, we used HIV envelope gp140 and CD4 or coreceptor (CoR) binding site (bs) mutant probes to evaluate HIV-specific responses in peripheral blood B cells of HIV-infected individuals at various stages of infection. In contrast to non-HIV responses, HIV-specific responses against gp140 were enriched within abnormal B cells, namely activated and exhausted memory subsets, which are largely absent in the blood of uninfected individuals. Responses against the CoRbs, which is a poorly neutralizing epitope, arose early, whereas those against the well-characterized neutralizing epitope CD4bs were delayed and infrequent. Enrichment of the HIV-specific response within resting memory B cells, the predominant subset in uninfected individuals, did occur in certain infected individuals who maintained low levels of plasma viremia and immune activation with or without antiretroviral therapy. The distribution of HIV-specific responses among memory B cell subsets was corroborated by transcriptional analyses. Taken together, our findings provide valuable insight into virus-specific B cell responses in HIV infection and demonstrate that memory B cell abnormalities may contribute to the ineffectiveness of the antibody response in infected individuals.

Introduction

A small number of human anti-HIV antibodies with modest neutralizing activity were identified prior to 2009, after which and in rapid succession, several broadly neutralizing antibodies (bNAbs) with potent activity were isolated from prescreened HIV-infected individuals (1–6). The methods used to screen and produce these novel bNAbs incorporated advances in HIV envelope protein engineering and a variety of technologies, including high-throughput screening of serum designed to measure HIV-neutralizing antibody activities (7–11). The cumulative data from these analyses also revealed that while the antibody response against HIV arises within weeks of acquisition of infection, these early antibodies are largely non-neutralizing and unlikely to contribute to the control of HIV replication (12). Furthermore, only after several years of HIV infection do a limited percentage, in the range of 10% to 30%, of untreated individuals develop serologic activities that are broadly neutralizing (9, 13). However, as responses broaden, whether from a single or a combination of bNAb specificities, they are nonetheless ineffective at clearing or controlling the virus in infected individuals from whom they are isolated (14).

Functional HIV envelope spikes are sparsely distributed over the surface of the virion, and each is composed of a trimer of noncovalently associated surface glycoprotein gp120 and transmembrane protein gp41 molecules (9, 11). This complex interacts with its primary receptor (CD4) and subsequently with a chemokine coreceptor (CoR) expressed on the surface of target cells. Both CD4 and CoR binding sites (bs) of gp120 are highly conserved and immunogenic, with immunogenicity being especially true of the latter site. All bNAbs that have been isolated thus far target the HIV envelope spike and have been classified into 4 categories that reflect sites targeted by the bNAbs; these include the CD4bs, the membrane proximal external region of gp41, as well as glycan-dependent sites in V1/V2 loops and the V3 loop of gp120 (7, 9, 11). The bNAbs directed against the CD4bs, all of which were generated with HIV envelope probes used to identify and sort HIV-specific B cells (3, 15), have been shown to be highly potent and possess similar features (3–5, 14, 16). However, such CD4bs bNAbs are thought to develop infrequently and only after several years of infection (9). In contrast, antibodies directed against the CoRbs emerge relatively early, yet few of these antibodies demonstrate neutralizing activity against HIV, likely at least in part because access to the CoRbs is restricted (17–20). Many of the recently isolated antibodies directed against the CD4bs have high levels of somatic mutation (3–5), a property that likely reflects prolonged affinity maturation of B cell clones.

While neutralizing antibodies have been extensively studied, and several hypotheses have been put forth to explain why bNAbs are not readily produced in infected individuals, very little is known regarding the nature of the B cells from which HIV-specific

Authorship note: Lela Kardava and Susan Moir contributed equally to this work.
Conflict of interest: The authors have declared that no conflict of interest exists.
Citation for this article: *J Clin Invest.* 2014;124(7):3252–3262. doi:10.1172/JCI74351.

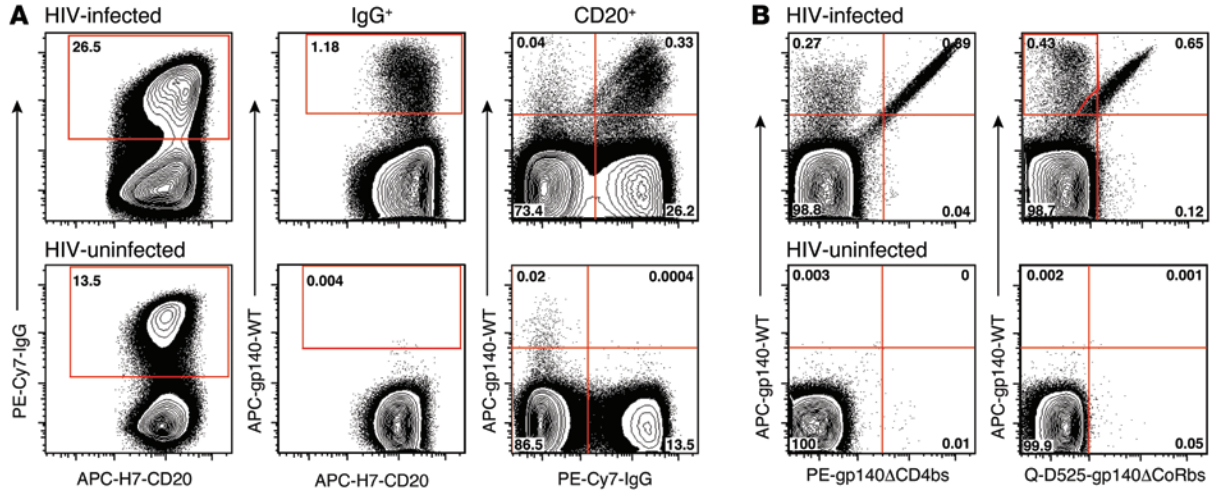

Figure 1

Identification of HIV-specific B cells by FACS analysis. Mature ($CD10^-$) B cells isolated from the peripheral blood of representative HIV-infected untreated and uninfected individuals and stained for CD20, IgG, and 3 gp140 probes. (**A**) Binding of gp140-WT probe to B cells shown by CD20 and IgG. (**B**) Binding of gp140-WT probe to B cells shown by gp140 probes with point mutations at CD4 (gp140ΔCD4bs) and CoR (gp140ΔCoRbs) bs. The numbers refer to the percentage of cells in each quadrant or the percentage of cells within the gated population relative to the total number of cells shown in the dot plot.

antibodies originate (7, 9–11). Although HIV does not productively infect B cells, numerous phenotypic and functional abnormalities of B cells have been described in HIV disease (21, 22). The indirect and persistent effects of ongoing HIV replication have been associated with aberrant B cell activation, increased B cell exhaustion, as well as deficiencies in the development of normal B cell memory (21). Whereas resting memory B cells represent the predominant memory subset in healthy individuals, their frequencies are reduced in almost all stages of HIV disease, regardless of treatment status (21, 22). In untreated HIV-viremic individuals, tissue-like and activated memory B cells are the predominant memory subsets, the former being associated with HIV-induced cellular exhaustion and the latter, apoptosis (21). In addition, there is evidence that HIV directly interacts with B cells through nonspecific mechanisms, such as binding of immune-complexed virions to the complement receptor CD21 or HIV envelope-mediated binding either to C-type lectin receptors or to nonconventional antigen-binding regions of surface Ig (23–26). Such nonspecific interactions may contribute to B cell hyperactivation, although these effects are thought to be largely polyclonal and not directed against HIV itself (27, 28). Nonetheless, an accurate assessment of the B cell receptor–mediated (BCR-mediated) response against HIV is needed in order to better understand the evolution of the HIV-specific antibody response after infection and why this response is so ineffective in infected individuals.

In the present study, we characterized HIV-specific memory B cell responses in infected individuals by direct methods using various HIV envelope probes designed to measure the total response as well as responses directed against the CD4bs or CoRbs of the envelope. Our results demonstrate that the majority of gp140-specific responses, including those against the conserved CD4bs, are found within abnormal B cell subsets, namely activated and exhausted memory B cells that are largely absent in the blood of HIV-negative individuals. These responses are highest during the early stage of HIV infection, significantly decreased following the initiation of antiretroviral therapy (ART), and most importantly, enriched in normal resting memory B cells when HIV viremia and immune activation are controlled either naturally or as a result of ART. These findings have potentially important implications in understanding the pathophysiologic mechanisms responsible for the defective antibody responses against HIV and the inability to readily produce bNAbs.

Results

HIV-specific B cell responses in early and chronically HIV-infected individuals. We used a trimerized, biotinylated, and fluoresceinated form of the WT HIV envelope gp140 from the primary B-clade isolate YU2 (henceforth referred to as gp140-WT probe) to identify HIV-specific B cells by flow cytometry. Analyses were restricted to B cells that expressed IgG in order to maximize BCR-binding measurements and minimize low-affinity non-BCR binding of the HIV envelope to B cells that can occur via various cell surface receptors, including several lectins and integrins (24, 26, 29). As shown by the representative profile in Figure 1A and consistent with published observations (15, 30), a low yet clearly discernible frequency of IgG^+ B cells in the peripheral blood of HIV-infected, but not uninfected, individuals bound the gp140-WT probe with high affinity. The diagonal patterns observed when gp140-WT and anti-IgG binding were displayed together suggested that these events represented IgG-containing BCRs that were specific, albeit of varying affinities, to the HIV envelope (Figure 1A). Low frequencies of IgG^- B cells also bound gp140, although patterns and levels were similar for both HIV-infected and uninfected individuals (Figure 1A). In order to determine the relative proportion of B cell binding to the gp140-WT probe that represented binding to CD4bs versus CoRbs, we performed mutational studies that allowed segregation of binding to these individual epitopes. In this regard, costaining of the gp140-WT probe with gp140 trimers containing a single-point mutation in the CD4bs or CoRbs yielded diagonal patterns in the upper-right quadrants that represented common

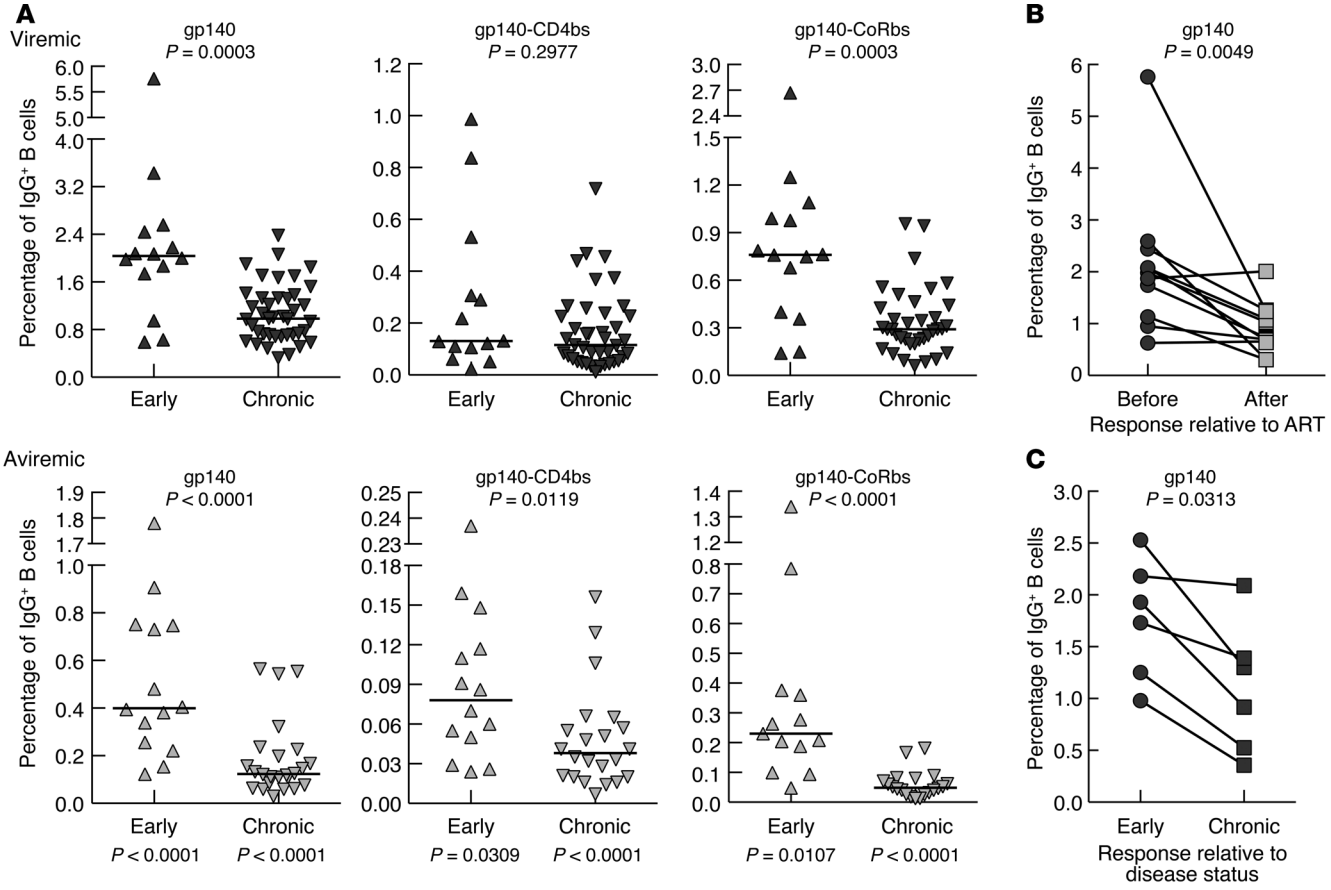

Figure 2

Frequencies of HIV-specific B cells in early and chronic HIV infection. (**A**) Cross-sectional FACS analysis of B cells from individuals at early and chronic phases of infection stained with gp140 probes. Top panels include untreated viremic individuals, and bottom panels include individuals who began ART during their early or chronic phase of infection and were aviremic at the time of analysis. Horizontal bars show median values, and *P* values below graphs represent comparisons between viremic and aviremic individuals for a corresponding early or chronic stage of infection. Longitudinal FACS analysis of gp140-WT binding to B cells of (**B**) HIV-infected individuals before and after reduction of viremia by ART and (**C**) HIV-viremic untreated individuals at early and later chronic phases of infection. Median time after initiation of ART was 18 months.

binding between gp140-WT and each mutated probe, as well as events in the upper-left quadrants that represented site-specific binding of 0.27% and 0.43% for gp140-CD4bs and gp140-CoRbs, respectively for the HIV-infected individual (Figure 1B). Binding of mutant probes to IgG$^+$ B cells of HIV-uninfected individuals was at background levels (Figure 1B). Of note, the HIV specificity of these probes was demonstrated by ELISA (Supplemental Figure 1; supplemental material available online with this article; doi:10.1172/JCI74351DS1) and by single-cell sorting, in which the vast majority of antibodies isolated from IgG$^+$ B cells using these probes were determined to be HIV specific (refs. 31, 32, and unpublished data). Collectively, these observations indicate that fluoresceinated gp140-WT trimer probes and mutant derivatives can be used in combination with anti-IgG to evaluate frequencies of HIV-specific IgG$^+$ B cells circulating in the peripheral blood of HIV-infected individuals.

We then used the 3 probes to measure frequencies of HIV-specific IgG$^+$ B cells at early or chronic phases of HIV infection in the peripheral blood of individuals who remained untreated (viremic) or who initiated ART during either of these 2 phases (aviremic). As shown in Figure 2A for cross-sectional analyses, we detected IgG$^+$ B cells specific to gp140-WT early after infection, and the median frequency of HIV-specific B cells in the early viremic group was significantly higher than that of the chronically viremic group. These differences extended to corresponding aviremic groups; however, reduction of plasma viremia by ART in early or chronic infection was also associated with significantly reduced frequencies of gp140-WT binding B cells when compared with untreated (viremic) counterparts (Figure 2A; note difference in scale). Longitudinal analyses combining individuals from both early and chronic groups confirmed that ART-mediated reduction in HIV plasma viremia was associated with decreased frequencies of HIV gp140–specific B cells (Figure 2B). Such frequencies were also significantly reduced by the transition from early to chronic phases of HIV infection in untreated individuals (Figure 2C); this effect was unlikely to be directly related to levels of HIV plasma viremia, given that viral loads were not significantly different at the 2 time points assayed (data not shown). We found that patterns of response to gp140-CD4bs and gp140-CoRbs were similar to those observed for gp140-WT, with 2 important exceptions. First, the frequencies of gp140-CD4bs–specific B cells were generally lower than those specific for gp140-CoRbs, especially in the early viremic group (Figure 2A).

Second, and related to the latter observation, we observed no significant difference in the frequencies of gp140-CD4bs–specific B cells between the early and chronic viremic groups (Figure 2A). These data are consistent with findings demonstrating that neutralizing antibodies directed against the CD4bs of the HIV envelope take long periods of time (often several years) to emerge (33). Collectively, these observations indicate that HIV-specific B cells arise early after infection and are blunted by ART-mediated reduction of HIV viremia or by the presence of chronic viremia itself; however, they are very poorly directed against at least 1 of the recognized broadly neutralizing epitopes on the HIV envelope, i.e., CD4bs.

HIV-specific responses among memory B cell subsets. We and others have previously shown that several subsets of antigen-experienced B cells, including IgG-switched B cells, can be identified in the peripheral blood, some of which do not express the classic marker of memory CD27 and several of which become over- or underexpressed in various disease settings, including HIV infection (21, 22). Accordingly, we sought to determine the distribution of HIV-specific B cells among various phenotypic and functional B cell subsets. Thus, mature IgG-expressing B cells were divided into 4 subsets based on expression of CD27 and CD21: 2 subsets that constituted the majority of B cells in healthy donors, namely $CD21^{hi}$-$CD27^{-}$ naive and $CD21^{hi}$-$CD27^{+}$ resting memory B cells, as well as 2 subsets abnormally overrepresented in HIV-viremic individuals (34), namely $CD21^{lo}$-$CD27^{-}$ tissue-like and $CD21^{lo}$-$CD27^{+}$ activated memory B cells (subset distribution shown in Supplemental Figure 2A). Of note, IgG-expressing B cells within the naive subset are often referred to as $CD27^{-}$ memory B cells (35). However, a different term was needed for clarity, given that tissue-like memory B cells also lack expression of CD27. As such, we chose the term "intermediate memory" for IgG-expressing $CD21^{hi}$-$CD27^{-}$ B cells, reflecting that these B cells have class switched, but may have undergone limited affinity maturation (36). The contribution of each subset to the HIV-specific B cell response with regard to total response ($gp140^{+}$), CD4bs specificity ($gp140\text{-}CD4bs^{+}$), and CoRbs ($gp140\text{-}CoRbs^{+}$) was then evaluated for the HIV-viremic individuals shown in Figure 2. Of note, while the frequencies of mature B cell subsets were clearly different, as previously reported (ref. 34 and Supplemental Figure 2A), among the 3 major memory B cell subsets in this cohort, the frequencies of IgG^{+} B cells were not significantly different (Supplemental Figure 2B). However, as shown by the representative plots in Figure 3A, the predominant binding to the gp140-WT probe was contained within the activated memory B cell subset (50.9%), followed by resting (31.2%) and tissue-like memory (16.1%) B cells, and finally, the smallest proportion was within intermediate memory B cells (1.82%). We observed a similar distribution from group analyses (Figure 3B); differences in binding to the gp140-WT probe between the subsets were significant, either by determining the proportional contribution of each subset to the binding (Figure 3) or the frequencies of binding within each subset (Supplemental Figure 2C). The subset distribution for the binding of IgG^{+} B cells to gp140 was also distinct from that of the total IgG^{+} B cells (Supplemental Figure 2D). When we examined binding to gp140-CD4bs by subset, it was found to be similar between activated and resting memory subsets and significantly higher in these 2 subsets when compared with binding in the other 2 subsets (Figure 3C). In contrast, responses against the CoRbs were similar in subset distribution to responses against gp140-WT in that they were predominated by the activated memory subset (Figure 3, C and B). Finally, "other" responses, representing binding to the remaining non-CD4bs and non-CoRbs among B cells that bound gp140-WT, were concentrated in resting and activated memory subsets, with a very low frequency in tissue-like memory B cells. In this regard, the proportion of tissue-like memory B cells that responded to the CD4bs was significantly increased when compared with that of the 2 other responses ($P < 0.0001$ for both CoRbs and "other").

Immune and virologic correlates of HIV-specific B cell responses. The pie charts shown in Figure 3 demonstrate that over 50% of the responses against gp140-WT and specific bs within the envelope were contained within subsets that are abnormal and are overrepresented in HIV-viremic individuals, namely activated and tissue-like memory B cells (34). However, the data also revealed that there was a wide range of responses within in each subset, suggesting individual variability. Numerous studies have shown that HIV disease progression is associated with deficiencies within the resting memory B cell compartment, both in terms of a reduction in numbers or frequencies of this subset as well as in defects in its functional attributes (reviewed in refs. 21, 22). In light of these observations, we determined whether the level of HIV viremia or various T cell subset parameters influenced the proportion of HIV-specific B cells contained within the resting memory B cell subset compared with the proportion of these cells in other examined subsets in untreated viremic individuals. As shown in Figure 4A, there were strong inverse correlations between the fraction of the gp140-WT–specific response contained within the resting memory B cell subset and both HIV plasma viremia and one of the most widely reported predictors of disease progression (37), namely, the frequency of $CD8^{+}$ T cells that express the activation marker CD38. However, there was no significant correlation between HIV-specific resting memory responses and $CD4^{+}$ T cell counts or percentages (Figure 4A). Finally, we evaluated the effect of reducing HIV plasma viremia by ART on the frequency (Figure 4B) and distribution (Figure 4C) of the HIV-specific response among B cell subsets for the longitudinal group shown in Figure 2B. ART-mediated reductions in HIV plasma viremia led to significant reductions in the frequencies of the HIV-specific response among tissue-like and activated, but not resting, memory B cells (Figure 4B). However, related to the reductions in the frequencies of HIV-specific responses among tissue-like and activated memory B cells, we observed significant relative increases and decreases in the fraction of the HIV-specific response contained within the resting and activated memory B cell subsets, respectively (Figure 4C). Of note, the frequencies of $CD8^{+}$ T cells expressing CD38 were also significantly reduced following ART (data not shown). Collectively, these observations indicate that the majority of the HIV-specific response is contained within the abnormal memory B cell subsets in most HIV-viremic individuals, whereas control of viremia, either naturally or due to effective ART, results in a relative enrichment of HIV-specific responses in resting memory B cells, a situation similar to that of antigen-specific responses seen in normal, HIV-uninfected individuals.

Distinct profiles for HIV-specific B cells. Flow cytometry–based probes have recently been developed or optimized to evaluate memory B cells specific to antigens of common vaccines, including influenza (38) and tetanus (39). We took advantage of these highly specific probes to compare IgG^{+} B cell reactivities against HIV and non-HIV antigens among 12 HIV-viremic individuals selected on the basis of their immunization histories (see details in Methods). As shown by the representative plots in Figure 5A, binding to each of the 3 antigen

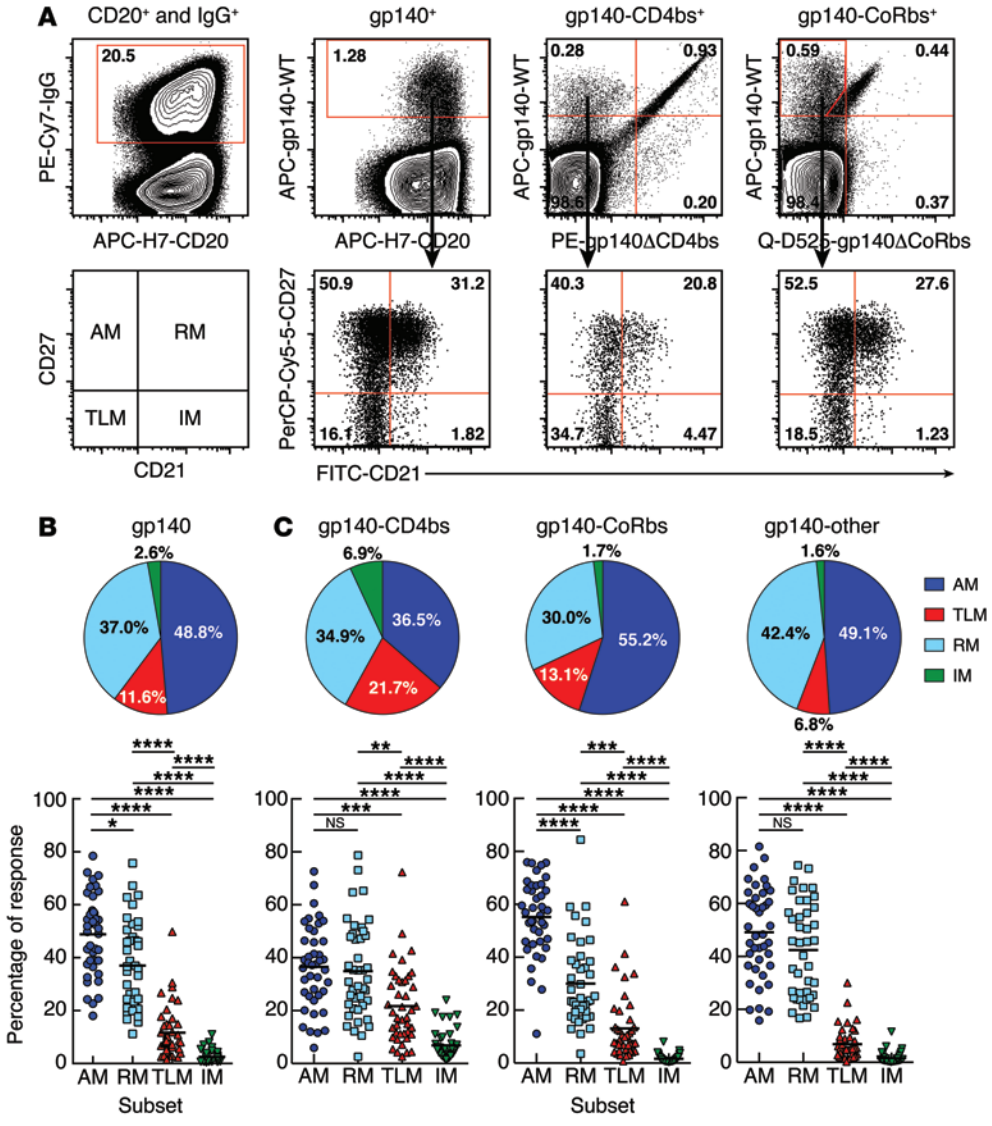

Figure 3

Frequencies of HIV-specific B cells by subset. (**A**) Mature ($CD10^-$) B cells isolated from the peripheral blood of a representative HIV-infected untreated individual and stained for CD20, IgG, CD21, CD27, and 3 gp140 probes. Gates were set on IgG^+ B cells, followed by gating on B cells that were positive for gp140, gp140-CD4bs, and gp140-CoRbs and displaying the expression of the probe-gated B cells by the subset-identifying markers CD21 and CD27. (**B**) Pie chart analysis of gp140-binding B cells by subset for 42 HIV-viremic individuals and comparison of gp140-binding frequencies between subsets. (**C**) Similar analyses as in **B**, but for epitope specificities within gp140 (CD4bs and CoRbs); "other" refers to responses to gp140 after subtraction of those specific to CD4bs and CoRbs. Horizontal bars show mean values. $^*P < 0.05$; $^{**}P < 0.01$; $^{***}P < 0.001$; $^{****}P < 0.0001$. The numbers in **A** refer to the percentage of cells in each quadrant or the percentage of cells within the gated population relative to the total number of cells shown in the dot plot. AM, activated memory; IM, intermediate memory; RM, resting memory; TLM, tissue-like memory.

probes was mutually exclusive when gates were set on high-intensity events, indicative of specificity; in cumulative analyses, frequencies of B cells binding gp140 were significantly higher compared with those binding influenza and tetanus (Figure 5B). Furthermore, binding of the 3 probes among the B cell subsets was different (Figure 5C). In addition, there were differences in binding patterns within each subset (Supplemental Figure 2E). Notably, we observed significantly more binding of activated memory B cells to gp140 compared with either influenza or tetanus, whereas there was significantly more binding of resting memory B cells to tetanus compared with that seen with the other 2 probes (Figure 5C). There were also differences within subsets that were distinct for each antigen. Binding to gp140, but not to influenza and tetanus, was significantly increased within the activated compared with the resting memory B cells, whereas the latter subset contained significantly increased frequencies of binding to gp140 and tetanus, but not to influenza when compared with the binding frequencies seen in tissue-like memory B cells (Supplemental Figure 2E). Collectively, these findings indicate that B cell responses against HIV (gp140) are clearly distinct from those against non-HIV antigens (influenza and tetanus).

Transcriptional profiles of HIV-specific B cells. The recent development and use of probes to characterize HIV-specific B cell responses by flow cytometry has provided new opportunities for investigating humoral immunity, although there are potential limitations, especially when subsets are involved, given the more subjective nature of these new phenotype-based analyses compared with the more conventional functional assays. Accordingly, we performed transcriptional analysis of HIV-specific B cells as a means of corroborating and extending the observations that HIV-specific responses are enriched within abnormal B cell subsets and that these responses are associated with and influenced by virologic and immunologic parameters. Given cell number limitations, we chose a high-sensitivity, low-density array approach to investigate transcriptional profiles of HIV-specific B cells. The array consisted of 29 genes representing several gene categories (Table 1) that were selected for their high likelihood of being differentially expressed in $CD21^{hi}$ (resting) versus $CD21^{lo}$ (tissue-like and activated) memory B cells. As shown in Table 1, the likelihood of being differentially expressed was estimated based on our preliminary data (microarray and single-gene RT-PCR data not shown) and several

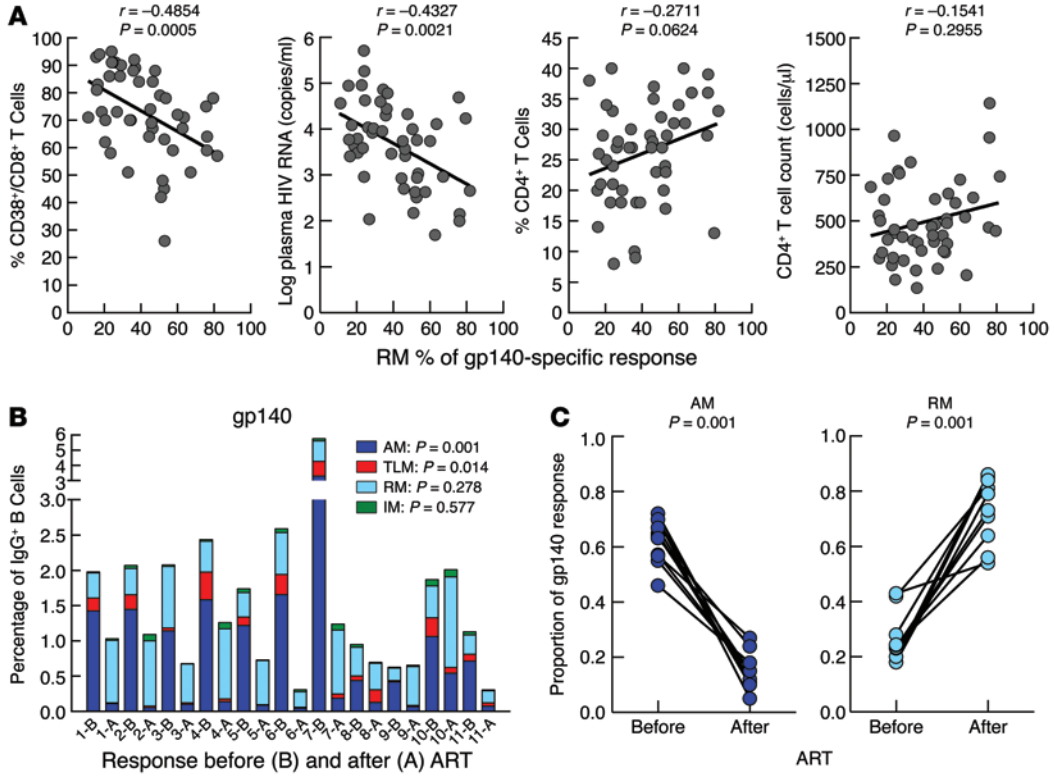

Figure 4
Immunologic and virologic associations with HIV-specific responses among resting memory B cells. (**A**) Correlations between the proportion of gp140-specific responses within resting memory B cells, and expression of CD38 on $CD8^+$ T cells, HIV plasma viremia, and $CD4^+$ T cell count or percentage in peripheral blood. Effects of reduction of HIV plasma viremia by ART on the (**B**) frequency and (**C**) distribution of the gp140-specific response among B cell subsets. The *P* values in **B** represent comparisons of frequencies before and after ART for each subset.

previous studies, in which $CD21^{lo}$ B cells or their exhausted T cell counterparts were shown to be distinct from other subsets by transcriptional and/or phenotypic analyses (40–45). When tested on memory B cell subsets isolated from the peripheral blood of chronically infected HIV-viremic individuals, the observed and predicted direction of change between $CD21^{hi}$ and $CD21^{lo}$ memory B cells was concordant for 26 of the 29 genes, although only 18 achieved statistical significance (Figure 6 and Table 1; false discovery rate [FDR] <10%). Among these 18 genes, 13 had lower expression in the resting memory B cells compared with that in the other 2 subsets, consistent with the findings of the studies used to design our panel of 29 genes (Table 1 and refs. 40–45). Conversely, and again consistent with these studies, the expression of the remaining 5 genes was higher in the resting memory B cells than in the other 2 subsets. Furthermore, hierarchical clustering analyses of the gene expression profiles showed robust separation among subsets, with tissue-like memory B cell profiles clustering together and distinct from those of resting memory B cells and activated memory B cells, with the latter 2 displaying more intermediate and less distinct clustering (Figure 6).

Finally, we evaluated whether the transcriptional profiles of HIV-specific B cells with distinct phenotypic and HIV disease properties were associated with the subset-specific profiles shown in Figure 6. Accordingly, gp140-specific IgG^+ B cells were sorted from individuals with either a strong or weak pro-resting memory profile, as shown in Figures 3 and 4, and their transcriptional profiles were compared with each other and in association with the subset profiles. We found that the expression of 14 of 29 genes was significantly different (Figure 6 and Supplemental Table 1) and that 10 of these 14 genes were among the 18 genes differentially expressed in the resting memory B cell subset; an additional 4 are known to be associated with virus-induced lymphocyte exhaustion and/or $CD21^{lo}$ B cells (43–45). Among these 14 genes are homing receptors, receptors with known or putative immunoregulatory roles, as well as proteins associated with lymphocyte signaling and immune responses (Figure 6 and Supplemental Table 1). Collectively, the transcriptional profiling confirmed and extended the observation that the distribution of HIV-specific response among the normal (resting) and abnormal (tissue-like and activated) memory B cells correlates with virologic and immunologic properties of HIV disease.

Discussion

In the present study, we have demonstrated that the HIV-specific B cell response as measured in the peripheral blood of infected untreated individuals is concentrated within abnormal B cell subsets, namely activated and tissue-like or exhausted memory B cells that are largely absent in healthy uninfected individuals. HIV-specific B cell responses were also clearly distinct from responses against the non-HIV antigens influenza and tetanus, the latter of which was comparatively enriched within the resting memory B cell subset. However, we also found that resting memory B cells, which are abundant in healthy uninfected individuals and depleted in HIV disease (21, 22, 46), accounted for a relatively greater proportion of the HIV-specific response in infected individuals who maintained low plasma viremia and low immune activation either naturally or as a result of the initiation of ART. Furthermore, the response against the highly immunogenic yet generally poorly neutralizing site, CoRbs, was strongest in early HIV infection, contrasting with a less rapid response against the less immunogenic yet more neutralizing site, CD4bs. This latter finding is consistent with reports that when broadly neutralizing antibody responses against the CD4bs arise, they do so only after years of infection (33).

Table 1
Low-density array gene analysis

Category	Gene names	Predicted expression[A]	Reference	Fold change[A]	FDR[C]	*P* value	Concordance[D]
Inhibitory receptors	*FCRL4*	Decreased	40, 41, 44	**–3.31**[B]	**0.006**	**2.05×10^{-3}**	**Yes**
	SIGLEC6	Decreased	43, 44	**–5.57**	**0.004**	**7.54×10^{-4}**	**Yes**
	FCGR2B	Decreased	43, 44	–1.34	0.376	2.91×10^{-1}	Yes
	LILRB1	Decreased	43, 44	–1.17	0.376	2.91×10^{-1}	Yes
	LILRB2	Decreased	43, 44	**–4.79**	**0.006**	**1.29×10^{-3}**	**Yes**
	CD72	Decreased	43, 44	–1.86	0.203	1.25×10^{-1}	Yes
	LAIR1	Decreased	44	–0.61	0.528	4.94×10^{-1}	Yes
	CD84	Decreased	41–43	**–2.79**	**0.021**	**9.70×10^{-3}**	**Yes**
	PTGER4	Decreased	45	0.83	0.502	4.37×10^{-1}	No
Cell activation	*SLAMF7*	Decreased	43	**–2.70**	**0.071**	**4.15×10^{-2}**	**Yes**
Trafficking	*ITGAX*	Decreased	43–45	**–5.54**	**0.006**	**2.05×10^{-3}**	**Yes**
	SELL	Increased	42–45	**3.82**	**0.012**	**4.74×10^{-3}**	**Yes**
	CCR7	Increased	43, 44	**3.62**	**0.016**	**6.90×10^{-3}**	**Yes**
Cytokine receptors	*IL13RA1*	Increased	42, 43	**2.60**	**0.071**	**4.15×10^{-2}**	**Yes**
	IL4R	Increased	42, 43, 45	1.21	0.376	2.91×10^{-1}	Yes
Tyrosine kinases and phosphatases	*HCK*	Decreased	40, 43	**–6.14**	**0.003**	**4.31×10^{-4}**	**Yes**
	LCK	Increased	40, 45	**5.21**	**0.003**	**4.31×10^{-4}**	**Yes**
	FGR	Decreased	40, 42	**–5.34**	**0.004**	**7.54×10^{-4}**	**Yes**
	FYN	Decreased	45	–1.05	0.416	3.35×10^{-1}	Yes
	PTPN22	Decreased	43	1.01	0.458	3.85×10^{-1}	No
	DUSP4	Decreased	40	–1.46	0.314	2.13×10^{-1}	Yes
Somatic hypermutation	*AICDA*	Decreased	40	**–4.07**	**0.006**	**2.05×10^{-3}**	**Yes**
Transcription factors	*PBX3*	Decreased	45	0.51	0.820	8.20×10^{-1}	No
	SOX5	Decreased	40, 42	**–3.00**	**0.028**	**1.35×10^{-2}**	**Yes**
	BCL11B	Decreased	43	**–7.53**	**0.003**	**1.08×10^{-4}**	**Yes**
Cell cycle	*CCNB2*	Decreased	40	–0.80	0.528	4.94×10^{-1}	Yes
Cell-cell signaling	*SEMA4A*	Decreased	45	**–6.31**	**0.003**	**4.31×10^{-4}**	**Yes**
Apoptosis	*TNFRSF1B*	Decreased	45	**–3.89**	**0.009**	**3.23×10^{-3}**	**Yes**
Cell anergy	*LAX1*	Increased	42	**3.47**	**0.035**	**1.82×10^{-2}**	**Yes**

[A]Predicted (based on the literature) or observed decrease or increase in $CD21^{hi}$ relative to $CD21^{lo}$ memory B cells. [B]Bold entries indicate genes whose expression was significantly different between $CD21^{hi}$ and $CD21^{lo}$ memory B cells. [C]Wilcoxon test followed by Benjamini-Hochberg FDR calculation. [D]Concordance between predicted and our observed change.

It is also noteworthy that the CD4bs is the target of many of the recently isolated potent bNAbs, including VRC01 and NIH45-46 (3, 4), yet in the majority of untreated HIV-viremic individuals in the present study, almost 60% of this response is contained within abnormal B cell subsets, either activated or exhausted.

Until recently, the only way to measure memory B cell responses against HIV was by inducing terminal differentiation in vitro with a polyclonal stimulus, followed by detection of HIV-specific antibodies or antibody-secreting cells by ELISA or ELISPOT, respectively (44, 47, 48). This approach required that HIV-specific B cells not only survive the in vitro culture period but also respond to the stimulation by undergoing terminal differentiation. There is good reason to believe that memory B cells of HIV-infected viremic individuals may be defective in these ex vivo processes, given their increased propensity to undergo apoptosis compared with memory B cells from HIV-uninfected and HIV-aviremic individuals (49–52). The recent development of trimeric HIV envelope probes that can measure directly HIV-specific B cells (15), without in vitro manipulation, represents a major advancement for studying humoral immunity against the virus. Such probes were critical to the success of many recent strategies aimed at identifying and isolating HIV envelope–specific human mAbs with highly potent and broad neutralizing activity against the virus (3–5, 16). In the present study, gp140 probes and their derivatives were also critical in demonstrating that the majority of the HIV envelope–specific response was contained within activated memory B cells, a subset shown previously to be highly prone to apoptosis in vitro and thus likely to have been undercounted by previous methods of analysis involving in vitro stimulation (34, 44, 48). Furthermore, the HIV probes can be combined with probes that bind non-HIV antigens such as influenza and tetanus. Our findings indicated clear distinctions between HIV and non-HIV B cell responses and suggested that antigens of vaccines, such as tetanus, to which individuals were exposed prior to becoming HIV infected, may be better maintained in the resting memory B cell compartment compared with antigens of HIV and, to a certain extent, with those of influenza.

However, the technique of directly evaluating HIV-specific B cell responses by HIV envelope probes also presents certain challenges and limitations, the most important being the fact that the HIV envelope can bind to non-BCR elements expressed on the surface of B cells or to nonconventional sites of the BCR itself (24–26, 29). While such binding cannot be completely eliminated, non-BCR–mediated binding of the HIV envelope to B cells can be minimized by a combination of costaining for IgG that creates a diagonal pattern of staining and by using B cells from HIV-uninfected individuals to determine where to set the gate between negative and likely

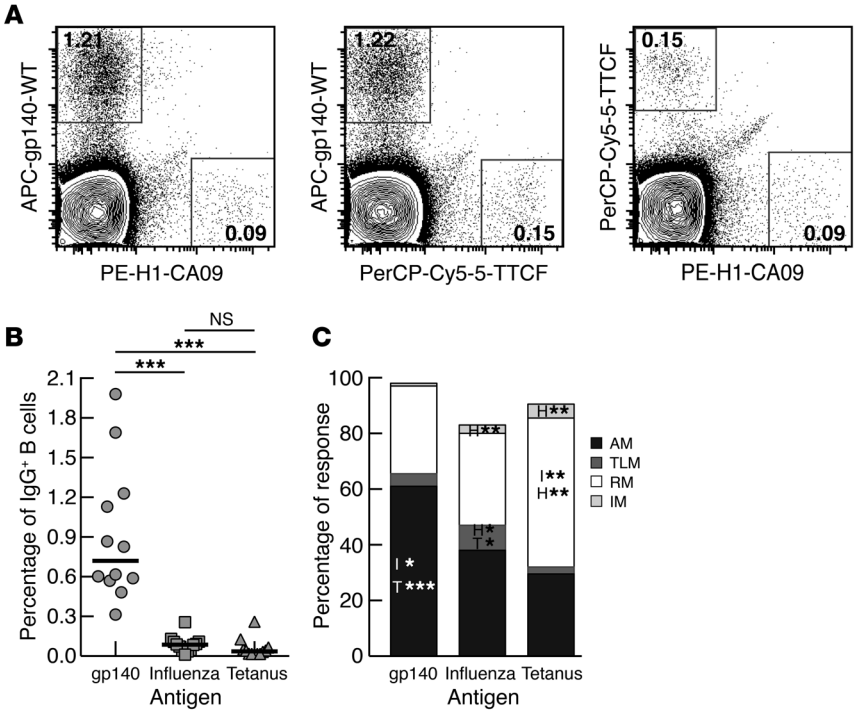

Figure 5

Comparisons between gp140-, influenza- and tetanus-specific B cells. Mature ($CD10^-$) B cells isolated from the peripheral blood of representative untreated HIV-infected individuals vaccinated with influenza or tetanus and stained for CD20, IgG, and 3 probes. (**A**) Binding of gp140, influenza (H1-CA09), and tetanus (TTCF) probes to B cells gated on CD20 and IgG. (**B**) Probe-binding frequencies shown by antigen for all IgG^+ B cells and (**C**) shown as median among each B cell subset. Horizontal bars show median values, and significant differences are identified in the subset with the higher value. $^*P < 0.05$; $^{**}P < 0.01$; $^{***}P < 0.001$. The numbers in **A** refer to the percentage of cells within the gated population relative to the total number of cells shown in the dot plot. I, influenza; T, tetanus; H, HIV gp140.

positive BCR-mediated staining. However, this strategy excludes HIV-specific B cells that have IgA- or IgM-based BCRs, the latter of which are enriched in tissue-like memory B cells (44, 53). Furthermore, IgG BCRs that recognize HIV envelope with low affinity, which are also likely to be more prevalent in the tissue-like memory B cell subset based on evidence of lower levels of somatic hypermutation compared with other memory B cell subsets (data not shown), would also be excluded from probe-based analyses.

Evaluation of antigen-specific memory B cell responses that is based exclusively on flow cytometry is also prone to more subjectivity than the more conventional functional analyses, especially when multiple fluorochromes are used to investigate subsets and subspecificities of antigen recognition. With regard to subset-based analyses, transcriptional profiling can both help identify distinct properties of the subsets involved and corroborate and extend observations made from phenotypic analyses. In this regard, we designed a 29-gene panel and used a low-density array approach to show distinctions between the 3 major IgG-expressing memory B cell subsets that circulate in the peripheral blood of HIV-viremic individuals and also to corroborate the flow-based observation that the HIV-specific B cell response of individuals with low viremia and low immune activation was primarily driven and maintained by resting memory B cells. We found that HIV-specific B cells with a predominantly resting memory phenotype have a transcriptional profile that is similar to that of the entire resting memory B cell subset, consistent with the expectation that HIV-specific B cells with a higher resting memory B cell frequency would be enriched for resting memory–specific genes. These included a relatively low expression of genes with potential negative immunoregulatory receptor–mediated (*SIGLEC6*, *CD72*, *CD84*, *FCRL4*, *LILRB1*, *FCGR2B*, and *LILRB2*) or signaling/transcriptional (*BCL11B*, *HCK*, *FYN*, *SOX5*, and *FGR*) effects (40, 42–45). Conversely, we found that higher HIV plasma viremia and immune activation, as reflected by increased frequencies of CD38-expressing $CD8^+$ T cells, were associated with an HIV-specific B cell response that was dominated by activated and tissue-like memory B cells. Given that activated memory B cells are highly prone to apoptosis (reviewed in ref. 21) and that tissue-like memory B cells are associated with exhaustion, including low proliferative capacity in vitro and in vivo (44), the observation that the HIV-specific response is enriched in these compartments in a majority of HIV-infected untreated individuals may help explain the inadequacy of the HIV-specific antibody response widely observed in these individuals. The observation that the contribution of the abnormal subset of activated memory B cells to the HIV-specific response was significantly diminished following ART, in contrast to that of the normal resting memory counterpart, is also consistent with the notion that the activated memory B cell subset is an unstable compartment that can only be maintained with active viral replication.

In summary, we used various probes in combination with markers that identify the major subsets of memory B cells circulating in the peripheral blood of HIV-infected individuals to assess the HIV and non-HIV–specific B cell responses in HIV disease. Higher levels of HIV viremia and immune activation were associated with HIV-specific responses that were enriched within abnormal B cell subsets, namely activated memory B cells that are highly prone to apoptosis and tissue-like memory that are associated with exhaustion. Conversely, non-HIV responses and HIV-specific responses associated with low levels of HIV viremia and immune activation, which resulted either from ART or from natural control of viral replication, were enriched in normal resting memory B cells, the predominant memory B cell subset in uninfected individuals. Given our previous findings that both the frequency and functionality of resting memory B cells are better preserved in early-treated individuals (34), our current findings provide an additional potential immunological benefit in facilitating the normalization of HIV-specific B cell responses by anti-HIV therapy. Thus, this study provides a pathophysiologic mechanism to explain, at least in part, the poor HIV-specific antibody response, particularly against an important neutralizing epitope on the HIV enve-

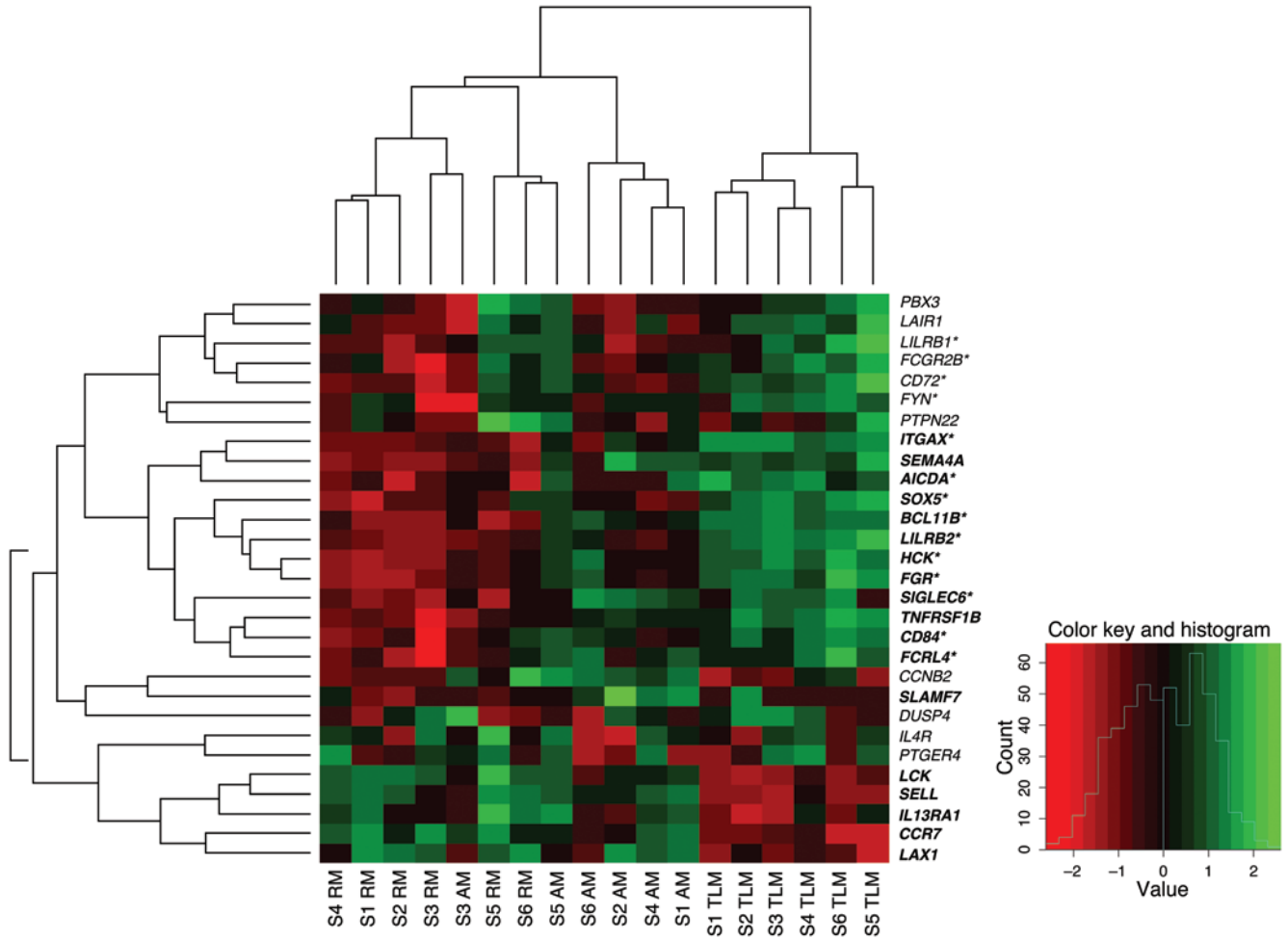

Figure 6
Transcriptional analysis by low-density array. Heatmap and hierarchical clustering of 29 genes and their levels of expression are shown for 3 sorted IgG+ memory B cell subsets from 6 HIV-viremic individuals (S1–S6). The subsets were resting, activated, and tissue-like memory B cells. Genes that were significantly different in expression between resting memory and the other 2 subsets are highlighted in bold. The asterisk identifies genes that were significantly different in expression between gp140-sorted IgG+ B cells of individuals with strong versus weak pro–resting memory profiles. An FDR of less than 10% was considered significant. Bootstrap and k-means clustering analyses were used to confirm that the separation of tissue-like memory samples from the rest (activated memory and resting memory) was highly robust.

lope, i.e., the CD4bs, and provides an additional scientific rationale for the early treatment of HIV-infected individuals for the purpose of reconstituting the HIV-specific antibody response within the normal resting memory B cell subset.

Methods

Study subjects. Leukapheresis products were obtained from HIV-infected individuals. Four groups of HIV-infected individuals were studied: early-infected HIV-viremic individuals, defined as having been infected within 6 months and not receiving ART; chronically infected HIV-viremic individuals, defined as having been infected for at least 6 months and not receiving ART; early-infected HIV-aviremic individuals, defined as having initiated ART during the early phase of infection and maintaining a plasma viremia level of fewer than 50 copies of HIV RNA per milliliter for at least 3 months; and chronically infected HIV-aviremic individuals, defined as having initiated ART during the chronic phase of infection and maintaining a plasma viremia level of fewer than 50 copies of HIV RNA per milliliter for at least 3 months. HIV plasma viremia was measured by branched DNA assay (Bayer Diagnostics), with a lower limit of detection of 50 copies per milliliter. A subcohort of 13 chronically infected HIV-viremic individuals was selected for assessment of B cell responses to influenza and tetanus vaccination. Median post-vaccination times for assayed samples were 4 months for tetanus (range 1–30 months) and 3 months for influenza (range 1–10 months).

Phenotypic analyses and cell sorting. PBMCs were obtained by density-gradient centrifugation and used fresh except for the samples for post-vaccination assays in which cryopreserved PBMCs were used. Mature ($CD10^-$) B cells were isolated from PBMCs by negative magnetic bead–based selection using a B cell enrichment cocktail (composed of antibodies against CD2, CD3, CD14, CD16, CD36, CD42b, CD56, CD66b, CD123, and glycophorin A) that was supplemented with tetrameric anti-CD10 mAb (STEMCELL Technologies). Purities were typically greater than 95%, and CD4-expressing cells were a negligible impurity that did not contribute to gp140 binding (Supplemental Figure 3). Phenotypic analyses were performed using the following mAbs: FITC-conjugated anti-human CD21 (Beckman Coulter); PerCP-Cy5.5– or

BV421-conjugated anti-human CD27, BV421-conjugated anti-CD4, and BV421- or BV510-conjugated anti-CD3 (BioLegend); and APC-H7–conjugated CD20 and PE-Cy7–conjugated anti-human IgG (BD Biosciences). HIV-specific memory B cells were identified using 3 trimeric HIV envelope gp140 probes: gp140-WT; a mutant gp140 probe with a single-point mutation in the CD4 binding region (D368R); and a mutant gp140 probe with a single-point mutation in the CoR binding region (I420R). All 3 probes contain a site-specific biotinylation motif Avi tag at the C termini and can be fluorescently labeled and used in flow cytometric analyses and cell sorting. Expression of these gp140 probes was performed as described previously (54). HIV-gp140-WT was conjugated with streptavidin-APC (Invitrogen), gp140-CD4bs mutant was conjugated with streptavidin-PE (Invitrogen), and gp140-CoRbs mutant was conjugated with streptavidin-Qdot525 (Invitrogen). CD4bs- or CoRbs-specific memory B cells were selected based on high-level recognition of gp140-WT glycoprotein and low-level recognition of the gp140-CD4bs mutant or CoRbs mutant as described previously (15, 20, 31, 55). Tetanus toxoid C-fragment and negative control CD80 tetramers were conjugated with streptavidin-PE (Invitrogen) or PerCP-Cy5.5 (BioLegend) as described previously (39). Only B cells that bound to the tetanus probe at a frequency that was 4-fold above that of binding to CD80 were included in the data set. Two PE-conjugated H1 influenza probes were used as previously described (38), one from H1 strain NC-99 for samples collected prior to the 2009-2010 season and one from CA-09 for samples collected during or after the 2009-2010 season. FACS analyses were performed on a FACSCanto II flow cytometer (BD Biosciences), with data analyses performed using FlowJo software (Tree Star Inc.). B cell subsets and HIV-specific B cells were sorted on a FACSAria instrument (BD Biosciences).

Low-density array. For transcriptional analyses of B cell subsets and HIV-specific B cells, a low-density array approach was used. The array consisted of 29 genes that were chosen from several different categories (Table 1). Total RNA was isolated from sorted B cell subsets and HIV-specific B cells using the RNeasy micro kit with on-column DNase digestion (QIAGEN), according to the manufacturer specifications. cDNA was synthesized, then preamplified with a pool of primers and probes (TaqMan Gene Expression Assay) for the genes in Table 1 and analyzed by quantitative real-time PCR using the Applied Biosystems 7500 Real-Time PCR system. Data were normalized to the housekeeping genes *POLRIIA* and *GAPDH* by a comparative ΔCt method. The Ct values from a given sample were converted to ΔCt values by subtracting the Cts from the number of PCR cycles ($n = 45$). To normalize across samples, the mean value of the housekeeping genes *POLRIIA* and *GAPDH* was subtracted from the Ct values within each sample. Differential expression analysis of resting memory B cells versus the other 2 subsets, namely tissue-like memory B cells and activated memory B cells, was performed using a 2-sample Wilcoxon test. To correct for multiple testing, FDRs were estimated using the Benjamini-Hochberg (BH) method (56). A 10% FDR cutoff was used to define significant genes. Similarly, differential expression analysis for samples obtained from individuals with high and low resting memory B cell profiles for gp140 binding was performed using the same procedure. Hierarchical clustering and heatmap visualization of memory B cell subsets were performed using the heatmap.2 function of gplots package (57) in R.Bootstrap hierarchical clustering analysis with 10,000 bootstrap replications was performed on the microarray data using the pvclust package (58) in R. The agglomerative method used in hierarchical clustering was "average," and the distance measure used was "correlation." A dendrogram with *P* values for each cluster from this analysis was then plotted (the "approximately unbiased" *P* values were in red, and the "bootstrap probability" were in green – see ref. 58 for details). K-means clustering (k = 1–10) followed by optimal cluster number assessment with silhouette widths (using the pamk function in the fpc package in R) were used to independently evaluate the robustness of clustering relationships (59). The low-density array data have been deposited in the NCBI's Gene Expression Omnibus (GEO GSE56499).

Additional statistical methods. Statistical analyses were performed using Prism software, version 6.0 for Mac (GraphPad Software). Two-group comparisons were performed using the Mann-Whitney *U* test (Figure 2A), and the Wilcoxon signed rank test was used for longitudinal comparisons (Figure 2, B and C, and Figure 4C). Four-way subset analyses for pie charts were performed using the 1-way ANOVA test followed by pairwise comparisons with the paired *t* test; 3-way (antigen) or 4-way (subset) analyses of immunized individuals were performed by the Friedman test followed by pairwise comparisons with the Wilcoxon signed rank test, as previously described (44). Spearman's rank method was used to test for correlation. A *P* value less than or equal to 0.05 was considered significant.

Study approval. The present study (protocol 02-I-0202) was reviewed and approved by the IRB of the NIAID, NIH. All subjects provided written informed consent for participation in the study.

Acknowledgments

We thank the patients for their willingness to participate in this study. We thank Shyam Kottilil for patient recruitment and care and Catherine Rehm and Sara Jones for specimen processing. This work was supported by the Intramural Research Program of the NIAID, NIH. Y. Li was supported by NIH/NIAID grant R01AI102766 and NIAID Development Grant P30AI36214, Center for AIDS Research (CFAR), University of California, San Diego. K. W. Wucherpfennig was supported by NIH grant P01 AI045757.

Received for publication November 19, 2013, and accepted in revised form April 10, 2014.

Address correspondence to: Susan Moir, NIH, 9000 Rockville Pike, Building 10, Room 6A02, Bethesda, Maryland 20892, USA. Phone: 301.402.4559; Fax: 301.480.0643; E-mail: smoir@niaid.nih.gov.

Brian H. Santich's present address is: Gerstner Sloan-Kettering Graduate School of Biomedical Sciences, New York, New York, USA.

Leo J.Y. Kim's present address is: Case Western Reserve University, Cleveland, Ohio, USA.

Emily E. Spurlin's present address is: University of South Alabama, Mobile, Alabama, USA.

1. Corti D, et al. Analysis of memory B cell responses and isolation of novel monoclonal antibodies with neutralizing breadth from HIV-1-infected individuals. *PLoS One*. 2010;5(1):e8805.
2. Walker LM, et al. Broad and potent neutralizing antibodies from an African donor reveal a new HIV-1 vaccine target. *Science*. 2009;326(5950):285–289.
3. Wu X, et al. Rational design of envelope identifies broadly neutralizing human monoclonal antibodies to HIV-1. *Science*. 2010;329(5993):856–861.
4. Scheid JF, et al. Sequence and structural convergence of broad and potent HIV antibodies that mimic CD4 binding. *Science*. 2011;333(6049):1633–1637.
5. Wu X, et al. Focused evolution of HIV-1 neutralizing antibodies revealed by structures and deep sequencing. *Science*. 2011;333(6049):1593–1602.
6. Walker LM, et al. Broad neutralization coverage of HIV by multiple highly potent antibodies. *Nature*. 2011;477(7365):466–470.
7. Burton DR, et al. A blueprint for HIV vaccine discovery. *Cell Host Microbe*. 2012;12(4):396–407.
8. Moir S, Malaspina A, Fauci AS. Prospects for an HIV vaccine: leading B cells down the right path. *Nat Struct Mol Biol*. 2011;18(12):1317–1321.
9. Kwong PD, Mascola JR. Human antibodies that neutralize HIV-1: identification, structures, and B cell ontogenies. *Immunity*. 2012;37(3):412–425.
10. McCoy LE, Weiss RA. Neutralizing antibodies to HIV-1 induced by immunization. *J Exp Med*. 2013;210(2):209–223.

11. Klein F, Mouquet H, Dosenovic P, Scheid JF, Scharf L, Nussenzweig MC. Antibodies in HIV-1 vaccine development and therapy. *Science*. 2013;341(6151):1199–1204.
12. Bonsignori M, et al. HIV-1 antibodies from infection and vaccination: insights for guiding vaccine design. *Trends Microbiol*. 2012;20(11):532–539.
13. Mikell I, Sather DN, Kalams SA, Altfeld M, Alter G, Stamatatos L. Characteristics of the earliest cross-neutralizing antibody response to HIV-1. *PLoS Pathog*. 2011;7(1):e1001251.
14. Liao HX, et al. Co-evolution of a broadly neutralizing HIV-1 antibody and founder virus. *Nature*. 2013;496(7446):469–476.
15. Scheid JF, et al. A method for identification of HIV gp140 binding memory B cells in human blood. *J Immunol Methods*. 2009;343(2):65–67.
16. Georgiev IS, et al. Delineating antibody recognition in polyclonal sera from patterns of HIV-1 isolate neutralization. *Science*. 2013;340(6133):751–756.
17. Labrijn AF, et al. Access of antibody molecules to the conserved coreceptor binding site on glycoprotein gp120 is sterically restricted on primary human immunodeficiency virus type 1. *J Virol*. 2003; 77(19):10557–10565.
18. Chen W, Zhu Z, Feng Y, Dimitrov DS. Human domain antibodies to conserved sterically restricted regions on gp120 as exceptionally potent cross-reactive HIV-1 neutralizers. *Proc Natl Acad Sci U S A*. 2008;105(44):17121–17126.
19. Li Y, et al. Mechanism of neutralization by the broadly neutralizing HIV-1 monoclonal antibody VRC01. *J Virol*. 2011;85(17):8954–8967.
20. Li Y, et al. HIV-1 neutralizing antibodies display dual recognition of the primary and coreceptor binding sites and preferential binding to fully cleaved envelope glycoproteins. *J Virol*. 2012;86(20):11231–11241.
21. Moir S, Fauci AS. Insights into B cells and HIV-specific B cell responses in HIV-infected individuals. *Immunol Rev*. 2013;254(1):207–224.
22. Amu S, Ruffin N, Rethi B, Chiodi F. Impairment of B cell functions during HIV-1 infection. *AIDS*. 2013;27(15):2323–2334.
23. Moir S, et al. B cells of HIV-1-infected patients bind virions through CD21-complement interactions and transmit infectious virus to activated T cells. *J Exp Med*. 2000;192(5):637–646.
24. He B, et al. HIV-1 envelope triggers polyclonal Ig class switch recombination through a CD40-independent mechanism involving BAFF and C-type lectin receptors. *J Immunol*. 2006;176(7):3931–3941.
25. Silverman GJ, Goodyear CS. Confounding B cell defences: lessons from a staphylococcal superantigen. *Nat Rev Immunol*. 2006;6(6):465–475.
26. Rappocciolo G, et al. DC-SIGN on B lymphocytes is required for transmission of HIV-1 to T lymphocytes. *PLoS Pathog*. 2006;2(7):e70.
27. Haas A, Zimmermann K, Oxenius A. Antigen-dependent and -independent mechanisms of T and B cell hyperactivation during chronic HIV-1 infection. *J Virol*. 2011;85(23):12102–12113.
28. Klasse PJ, Sanders RW, Cerutti A, Moore JP. How can HIV-type-1-Env immunogenicity be improved to facilitate antibody-based vaccine development? *AIDS Res Hum Retroviruses*. 2012;28(1):1–15.
29. Jelicic K, et al. The HIV-1 envelope protein gp120 impairs B cell proliferation by inducing TGF-beta1 production and FcRL4 expression. *Nat Immunol*. 2013;14(12):1256–1265.
30. Kobie JJ, et al. 9G4 autoreactivity is increased in HIV-infected patients and correlates with HIV broadly neutralizing serum activity. *PLoS One*. 2012; 7(4):e35356.
31. Sundling C, et al. High-resolution definition of vaccine-elicited B cell responses against the HIV primary receptor binding site. *Sci Transl Med*. 2012;4(142):142ra96.
32. Scheid JF, et al. Broad diversity of neutralizing antibodies isolated from memory B cells in HIV-infected individuals. *Nature*. 2009;458(7238):636–640.
33. Lynch RM, et al. The development of CD4 binding site antibodies during HIV-1 infection. *J Virol*. 2012;86(14):7588–7595.
34. Moir S, et al. B cells in early and chronic HIV infection: evidence for preservation of immune function associated with early initiation of antiretroviral therapy. *Blood*. 2010;116(25):5571–5579.
35. Kaminski DA, Wei C, Qian Y, Rosenberg AF, Sanz I. Advances in human B cell phenotypic profiling. *Front Immunol*. 2012;3:302.
36. Berkowska MA, et al. Human memory B cells originate from three distinct germinal center-dependent and -independent maturation pathways. *Blood*. 2011;118(8):2150–2158.
37. Lackner AA, Lederman MM, Rodriguez B. HIV pathogenesis: the host. *Cold Spring Harb Perspect Med*. 2012;2(9):a007005.
38. Whittle JR, et al. Flow cytometry reveals that H5N1 vaccination elicits cross-reactive stem-directed antibodies from multiple Ig heavy chain lineages. *J Virol*. 2014;88(8):4047–4057.
39. Franz B, May KF Jr, Dranoff G, Wucherpfennig K. Ex vivo characterization and isolation of rare memory B cells with antigen tetramers. *Blood*. 2011;118(2):348–357.
40. Ehrhardt GR, Hijikata A, Kitamura H, Ohara O, Wang JY, Cooper MD. Discriminating gene expression profiles of memory B cell subpopulations. *J Exp Med*. 2008;205(8):1807–1817.
41. Ehrhardt GR, et al. Expression of the immunoregulatory molecule FcRH4 defines a distinctive tissue-based population of memory B cells. *J Exp Med*. 2005;202(6):783–791.
42. Charles ED, et al. Clonal B cells in patients with hepatitis C virus-associated mixed cryoglobulinemia contain an expanded anergic CD21low B cell subset. *Blood*. 2011;117(20):5425–5437.
43. Isnardi I, et al. Complement receptor 2/CD21- human naive B cells contain mostly autoreactive unresponsive clones. *Blood*. 2010;115(24):5026–5036.
44. Moir S, et al. Evidence for HIV-associated B cell exhaustion in a dysfunctional memory B cell compartment in HIV-infected viremic individuals. *J Exp Med*. 2008;205(8):1797–1805.
45. Wherry EJ, et al. Molecular Signature of CD8(+) T Cell Exhaustion during Chronic Viral Infection. *Immunity*. 2007;27(4):670–684.
46. Tarlinton D, Good-Jacobson K. Diversity among memory B cells: origin, consequences, and utility. *Science*. 2013;341(6151):1205–1211.
47. Conge AM, et al. Impairment of B-lymphocyte differentiation induced by dual triggering of the B cell antigen receptor and CD40 in advanced HIV-1-disease. *AIDS*. 1998;12(12):1437–1449.
48. De Milito A, et al. Mechanisms of hypergammaglobulinemia and impaired antigen-specific humoral immunity in HIV-1 infection. *Blood*. 2004;103(6):2180–2186.
49. Moir S, et al. Decreased survival of B cells of HIV-viremic patients mediated by altered expression of receptors of the TNF superfamily. *J Exp Med*. 2004;200(5):587–599.
50. van Grevenynghe J, et al. Loss of memory B cells during chronic HIV infection is driven by Foxo3a- and TRAIL-mediated apoptosis. *J Clin Invest*. 2011;121(10):3877–3888.
51. Titanji K, et al. Low frequency of plasma nerve-growth factor detection is associated with death of memory B lymphocytes in HIV-1 infection. *Clin Exp Immunol*. 2003;132(2):297–303.
52. Samuelsson A, Brostrom C, van Dijk N, Sonnerborg A, Chiodi F. Apoptosis of CD4+ and CD19+ cells during human immunodeficiency virus type 1 infection — correlation with clinical progression, viral load, and loss of humoral immunity. *Virology*. 1997;238(2):180–188.
53. Kardava L, et al. Attenuation of HIV-associated human B cell exhaustion by siRNA down-regulation of inhibitory receptors. *J Clin Invest*. 2011;121(7):2614–2624.
54. Li Y, et al. Analysis of neutralization specificities in polyclonal sera derived from human immunodeficiency virus type 1-infected individuals. *J Virol*. 2009;83(2):1045–1059.
55. Dosenovic P, et al. Selective expansion of HIV-1 envelope glycoprotein-specific B cell subsets recognizing distinct structural elements following immunization. *J Immunol*. 2009; 183(5):3373–3382.
56. Benjamini Y, Hochberg Y. Controlling the false discovery rate — a practical and powerful approach to multiple testing. *J Roy Stat Soc B Met*. 1995;57(1):289–300.
57. Warnes GR, Bolker B, Lumley T. *gplots: Various R Programming Tools For Plotting Data*. R package version 2.6.0. CRAN; 2014.
58. Suzuki R, Shimodaira H. Pvclust: an R package for assessing the uncertainty in hierarchical clustering. *Bioinformatics*. 2006;22(12):1540–1542.
59. Rousseeuw PJ. Silhouettes: A graphical aid to the interpretation and validation of cluster analysis. *J Comput Appl Math*. 1987;20:53–65.